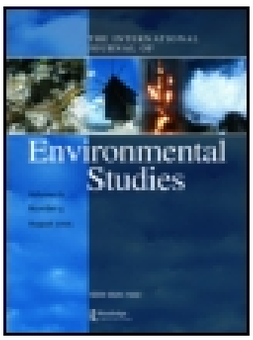

International Journal of Environmental Studies

ISSN: 0020-7233 (Print) 1029-0400 (Online) Journal homepage: http://www.tandfonline.com/loi/genv20

Layered double hydroxide of cobalt-zinc-aluminium intercalated with carbonate ion: preparation and Pb(II) ion removal capacity

Cyprian Y. Abasi, Paul N.E. Diagboya & Ezekiel D. Dikio

To cite this article: Cyprian Y. Abasi, Paul N.E. Diagboya & Ezekiel D. Dikio (2018): Layered double hydroxide of cobalt-zinc-aluminium intercalated with carbonate ion: preparation and Pb(II) ion removal capacity, International Journal of Environmental Studies, DOI: 10.1080/00207233.2018.1517935

To link to this article: https://doi.org/10.1080/00207233.2018.1517935

Published online: 24 Sep 2018.

INTERNATIONAL JOURNAL OF ENVIRONMENTAL STUDIES
https://doi.org/10.1080/00207233.2018.1517935

Routledge
Taylor & Francis Group

ARTICLE

Layered double hydroxide of cobalt-zinc-aluminium intercalated with carbonate ion: preparation and Pb(II) ion removal capacity

Cyprian Y. Abasi, Paul N.E. Diagboya and Ezekiel D. Dikio

Applied Chemistry and Nanoscience Laboratory, Department of Chemistry, Vaal University of Technology, Vanderbijlpark, South Africa

ABSTRACT

Ternary layered double hydroxide (Co–Zn–Al LDH) intercalated with carbonate was synthesised via a simple co-precipitation method at pH ≥10. It was characterised using the Fourier transform infrared (FTIR) spectrometer, *X*-ray diffractometer (XRD), surface area and porosity analyser, Thermo-gravimetric/differential thermal analysis (TGA–DTA), and Scanning Electron Microscope (SEM). The Pb(II) adsorption properties, mechanism, and possible reuse of the LDH were also investigated by the batch technique. The characterisation results showed the presence of hydroxyl group as well as the intercalated carbonate anions within the well-defined LDH crystal structure. The TGA-DTA results confirmed the presence of these anionic groups which were liberated from the structure at ≈200 and 300°C, respectively. The LDH-specific surface area, pore diameter and width are 54.0 m^2/g, 41.3 and 25.1 nm, respectively. Adsorption results showed that Pb(II) equilibrium could be achieved in 120 min, and adsorption increased with concentration and temperature. A Pb(II) adsorption capacity of 130.34 mg/g was reached for this LDH, and the adsorption process was spontaneous, endothermic and mainly electrostatic with most of the adsorption occurring within the pores. Desorption test suggested that approximately 90% of the adsorbed Pb(II) could be desorbed; hence, the Co–Zn–Al–CO_3 LDH may be reused.

KEYWORDS

Characterisation; adsorption; kinetic; adsorption isotherms; thermodynamics

Introduction

Water pollution, especially by toxic metals, is a worldwide problem. About one-third of the global population lacks reliable access to clean water [1–5]. Although several water treatment methods, such as membrane filtration, ion exchange, reverse osmosis, electrochemical treatment and adsorption-based techniques, have been employed in the past, adsorption-based techniques have been dominant, because of their various benefits. These include their environment-friendly character, the low-cost of materials and processing, ease of application and their tuneable absorbent properties [1,2,6,7]. Nevertheless, the search for readily available, more efficient and cheaper adsorbents continues.

CONTACT Ezekiel D. Dikio ezekield@vut.ac.za

Published online 24 Sep 2018

There is a growing interest in the adsorption chemistry of a group of synthetic anionic clays known as the layered double hydroxides (LDH) (also called hydrotalcite-like compounds) because of their potential for application in aqueous anionic and cationic pollutants adsorption [3,4,8,9]. This interest stems from the fact that LDHs have host-guest structures which consist of positively charged metal oxide/hydroxide sheets with intercalated anions and water molecules. They can be found in nature as well as obtained synthetically, and they are usually represented as $[M_{1-x}^{2+}M_x^{3+}(OH)_2](A^{n-})_{x/n} \cdot mH_2O$ where M^{2+} is a divalent metal cation and M^{3+} is a trivalent metal cation [10]. Owing to the partial substitutions of M^{3+} for M^{2+}, the hydroxide sheets are positively charged and require the intercalation of anions (A^{n-}) to retain the overall charge neutrality [3,8,10]. Generally, the various cations and anions may be replaced resulting in the alteration of their physical and chemical properties. This has led to the synthesis of LDH with remarkable properties such as high specific surface area, large pore size, an abundant repertory of surface functional groups, good thermal stability, high adsorption capacity and excellent regenerability [5,9].

Layered double hydroxides have been widely studied as catalysts, flocculants or other matrix materials because of their exchangeable interlayer anions and 'memory effect' [5,8]. Yet there have been surprisingly few studies on their use as adsorbents for water treatment [4,5,8]. Most studies have been on the binary LDH derivatives. Although the binary and ternary LDH have similar microstructure, the ternary LDH exhibit superior physicochemical properties owing to their higher and complex element composition. Hence, the aim of this study was to synthesise a trimetal composite Co–Zn–Al–CO_3 LDH for use as an adsorbent for the uptake of Pb(II) ions in aqueous solution. The synthesised Co–Zn–Al–CO_3 LDH composite adsorbent has been characterised, and the adsorption data have been explained using various models.

Materials and methods

Materials

Analytical grade reagents were used throughout this study. Cobalt nitrate hexahydrate [$Co(NO_3)_2.6H_2O$] (Riedel-deHaen, Germany), Zinc nitrate hexahydrate [$Zn(NO_3)_2.6H_2O$] (Merck, Germany), Aluminium nitrate nonahydrate [$Al(NO_3)_3.9H_2O$], Sodium carbonate (Na_2CO_3) and Sodium hydroxide (NaOH) (Sigma–Aldrich, Germany) were used without further purification.

Synthesis and characterisation of the LDH

The Co–Zn–Al–CO_3 LDH intercalated with carbonate was synthesised by the chemical co-precipitation method at pH ≥10. Typically, a mixed solution (400 mL) containing $Co(NO_3)_2.6H_2O$ (0.02M), $Zn(NO_3)_2.6H_2O$ (0.02M) and $Al(NO_3)_3.9H_2O$ (0.02 M) was added dropwise to vigorously stirred mixed solution (400 mL) of NaOH (0.1 M) and Na_2CO_3 (0.02 M) at 40°C. The resulting gel was aged for 21 h under continuous stirring to allow for crystal growth. The crystals were then washed repeatedly with deionised water by centrifuging at 4000 rpm for 5 min., followed by drying at 90°C for 17 h. The final product was called Co–Zn–Al–CO_3 LDH.

The as-synthesised Co–Zn–Al–CO_3 LDH was characterised by determining the associated functional groups using Fourier transform infrared (FTIR) spectrometer (Spectrum Two, Perkin Elmer Instruments, USA) in the scanning range of 400–4000 cm^{-1}, crystalline nature using *X*-ray diffractometer (XRD-7000, Shimadzu, Japan), and surface area and porosity using the Micromeritics TRISTAR II 3020 analyser (Micromeritics Instrument Corporation, USA). The Thermo-gravimetric analysis (TGA) was carried out using a PerkinElmer TGA 4000 (PerkinElmer Instruments, USA) using a heating rate of 10°C min^{-1}, and surface morphology using Zeiss Auriga Field Emission Scanning Electron Microscope (SEM) with an Oxford X-max EDX detector.

Batch adsorption experiments

Analytical grade lead nitrate ($Pb(NO_3)_2$) was used for stock solution (500 mg/L) preparation in this study. The effects of the following operating variables on Pb(II) uptake by Co–Zn–Al–CO_3 LDH were studied: time (1–120 min; Pb(II) concentration of 40 mg/L), pH (3–8; 40 mg/L of Pb(II) with shaking for 120 min), concentration (20–140 mg/L while shaking for 120 min), and temperature (25–65°C; 40 mg/L of Pb(II) with shaking for 120 min). Typically, 20 mg of the adsorbent was weighed into a polyethylene bottle, and 20 mL of the Pb(II) solution was added followed by incubation in a shaker at 200 rpm for the required time. Where necessary, the pH of working solutions was adjusted by adding drops of either 0.1 M HCl or NaOH. After the incubation, appropriate bottles were withdrawn from the shaker, and centrifuged at 4000 rpm for 5 min, and the concentration of Pb(II) ion left in the supernatant was determined using flame atomic absorption spectrophotometer (F-AAS, Shimadzu AA-7000, Japan).

The reusability of the adsorbent was tested by using 0.02 g of the Co–Zn–Al–CO_3 LDH composite and 10 mg/L. The adsorbent–pollutant mixtures were equilibrated at 200 rpm for 120 min at room temperature. At equilibrium, the bottles were withdrawn from the shaker, centrifuged at 4000 rpm for 5 min and the concentration of Pb(II) ion left in the supernatant determined as above. The residues from this experiment were carefully collected and desorbed in 20 mL of 0.01 M HCl by agitating for 120 min at 200 rpm. This was followed by centrifugation and determination of the desorbed Pb(II) ion as stated above.

Pb(II) adsorption data analysis

The quantity, q_e (mg/g), of Pb(II) ion adsorbed was determined using the material balance equation (Equation (1)) where v and m are the volume of the cation solution (L) and adsorbent mass (g), while C_o and C_e are the initial and final cation concentrations in solutions (mg/L), respectively.

$$q_e = (C_o - C_e)v/m \tag{1}$$

The equilibrium adsorption data were analysed using both two- and three-parameter adsorption isotherm models: Langmuir (Equation (2)), Freundlich (Equation (4)), Temkin (Equation (5)), Dubinin-Radushkevich (Equation (6)), Redlich-Peterson

(Equation (8)), and Sip's models (Equation (9)). The Langmuir adsorption isotherm model is given as

$$q_e = \frac{Q_o b C_e}{1 + bC_e} \tag{2}$$

where Q_o is the maximum adsorption capacity per unit weight of adsorbent, b is a solute–surface interaction energy-related parameter, q_e and C_e are same as above.

The Freundlich adsorption isotherm is given in Equation (3).

$$q_e = k_F C_o{}^{1/n} \tag{3}$$

where k_F is the Freundlich isotherm constant and n is the model linearity parameter.

The Temkin adsorption isotherm plot is given in Equation (4).

$$q_e = \frac{RT}{b_T} In(K_T C_o) \tag{4}$$

Where K_T is the Temkin adsorption isotherm constant ($dm^3\ g^{-1}$) and b_T is the adsorption potential of the adsorbent (J mol^{-1}).

The prevalent type of adsorption from the mean free energy E was determined using the Dubinin–Radushkevich in Equation (5)

$$q_e = q_D \exp(-B_D[RT \ln(1 + 1/C_e)]^2) \tag{5}$$

The mean free energy of sorption E is related to the constant B_D by the Equation (6).

$$E = \frac{1}{\sqrt{2B_D}} \tag{6}$$

The thermodynamic parameters – enthalpy change (ΔH^o) and entropy change (ΔS^o) – were obtained using the van't Hoff's Equation (7).

$$LnK_o = \frac{\Delta S^o}{R} - \frac{\Delta H^o}{RT} \tag{7}$$

The Gibbs free energy of sorption ΔG^o, which is a fundamental criterion for spontaneity, was obtained from Equation (8).

$$\Delta G^o = -RTLnK_o \tag{8}$$

The kinetic modelling of the adsorption of Pb(II) ions on the LDH was determined using the first-order (9), pseudo-first order (10), pseudo-second order (11) and Elovich (12) kinetic models, as well as the Weber-Morris [11] intra-particle diffusion model (13).

$$q_t = q_0 e^{-k_1 t} \tag{9}$$

$$q_t = q_e(1 - e^{-k_2 t}) \tag{10}$$

$$q_t = \frac{q_e^2 k_2 t}{1 + q_e k_2 t} \tag{11}$$

$$q_t = \frac{1}{\beta} In(\alpha\beta) + \frac{1}{\beta} In(t) \tag{12}$$

$$q_e = k_{IPD} t^{1/2} + C \tag{13}$$

Results and discussion

Characterisation studies

Figures 1 and 2 show the results of the various characterisations. Figure 1(a) shows the FTIR spectra peaks between 4000 and 450 cm^{-1} for the synthesised Co–Zn–Al–CO_3 LDH. The broadband around 3384 cm^{-1} has been assigned to stretching and bending vibrations of –OH groups lying within and on the surface of the LDH sheets [12,13]. The peak at 1356 cm^{-1} was attributed to the anti-symmetric stretching vibrations of C–O bond of the carbonate anion, while the bands between 790 and 551 cm^{-1} were assigned to the Al–O condensed groups, the Zn/Al–OH translation, and possibly the Al–OH deformation [5].

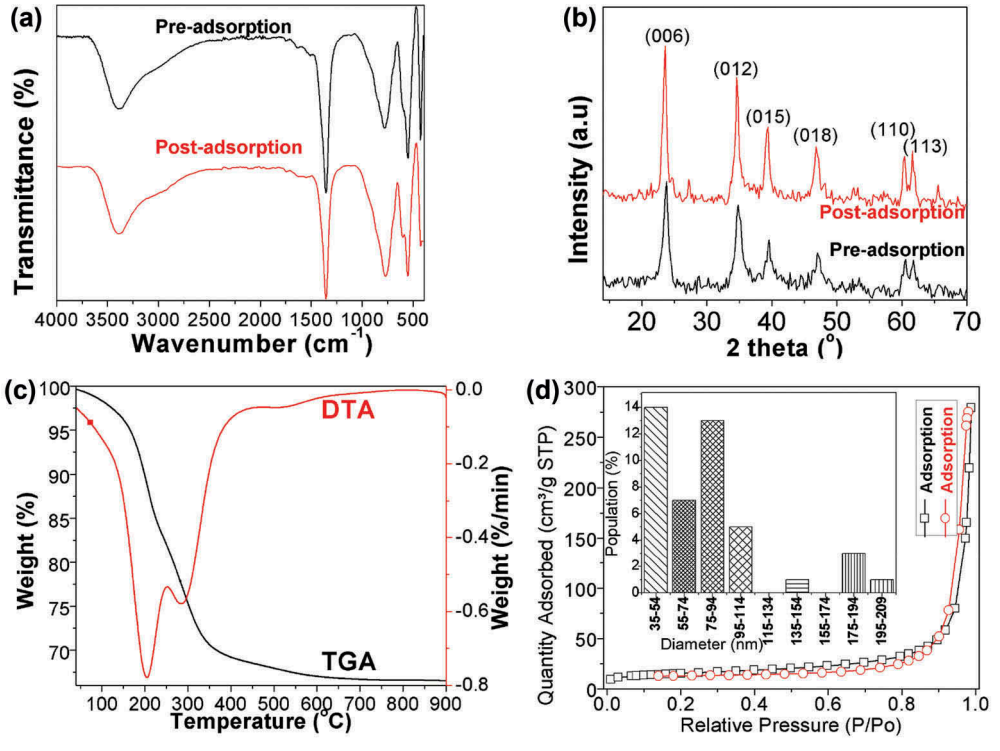

Figure 1. (a) FTIR and (b) XRD spectra of Co–Zn–Al LDH composite pre- and post-Pb(II) adsorption; (c) TGA/DTA spectra of the pristine Co–Zn–Al LDH composite; (d) Nitrogen adsorption-desorption isotherms of the pristine Co–Zn–Al LDH composite (Insert: Particle size distribution of the pristine Co–Zn–Al LDH).

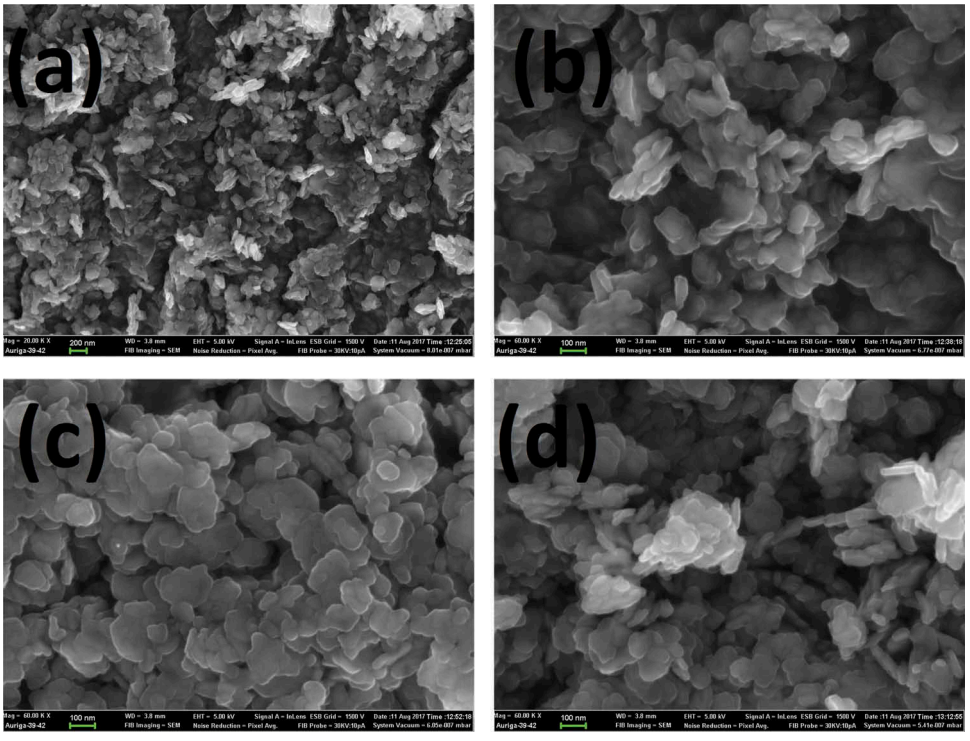

Figure 2. SEM images of the Co–Zn–Al LDH composite pre- (a and b) and post- (c and d) Pb(II) adsorption.

Figure 1(b) shows the powder *X*–ray diffractogram of the synthesised Co–Zn–Al–CO_3 LDH. The diffractogram exhibited characteristic polycrystalline peaks of the pristine LDH at 2θ values of 23.8 (006), 34.8 (012), 39.6 (015), 47.0 (018), and the doublet at 60.5 (110) and 61.8 (113). These peaks indicate the polycrystalline structure of the LDH. The post-adsorption *X*–ray diffractogram of the Co–Zn–Al–CO_3 LDH exhibited similar 2θ values but showed marked differences in peak intensities (higher); this suggested the introduction of the exogenous Pb(II) ions within the Co–Zn–Al–CO_3 LDH crystal structure [5,13]. The particle size distribution of the Co–Zn–Al–CO_3 LDH (Figure 1(d) insert) suggested that the major size distribution lay within the 76–165 nm range.

Thermo-gravimetric analysis (Figure 1(c)) showed two major thermal transition stages of the Co–Zn–Al–CO_3 LDH composite as the temperature increased from about 40°C to 900°C. The first was an endothermic decomposition which occurred from about 140°C to 210°C and was attributed to the initial loss of water on the interlayer and later to loss of hydroxyl groups on the lamella or dehydroxylation. The second endothermic decomposition occurred from 260°C to 320°C and was ascribed to loss of CO_2 of the carbonate anion [14,15]. A final decomposition of the CO_2 was observed about 490°C and 560°C. A total weight loss of approximately 33% at 600°C was attributed to the loss of entire water, hydroxyl and carbonate constituents in the pristine Co–Zn–Al–CO_3 LDH composite.

The BET-specific surface area obtained from the nitrogen adsorption-desorption isotherm of the pristine Co–Zn–Al–CO_3 LDH composite (Figure 1(d)) is 54.01 m^2/g, with a pore diameter of 41.34 nm and width of 25.14 nm. The shape of the adsorption-desorption suggests a type IV mesoporous adsorption isotherm with a characteristic type H3 hysteresis loop [16]. The H3 hysteresis loop indicates aggregates or loose assemblages of plate-like particles forming slit-like pores [17] as observed in the SEM images below (Figure 2).

Figure 2 shows the SEM images of pre/post adsorption Co–Zn–Al–CO_3 LDH adsorbent. The images showed agglomerated layered crystals characteristic of hydrotalcite-like compounds. Figure 3 shows energy dispersive spectroscopy (EDX) of the Co–Zn–Al–CO_3 LDH before and after adsorption studies. The percentage elemental distribution suggested close values between Co(II) and Zn(II), which confirmed that equimolar amounts of both elements participated in the synthesis. The nearly even distribution of both elements also indicated that their hydroxides were formed [18]. The post-adsorption EDX analysis showed the presence of the adsorbed Pb(II) with the Co–Zn–Al–CO_3 LDH composite, a confirmation that the synthesised adsorbed interacted with the aqueous Pb(II) ions.

Adsorption studies

Effect of time

Figure 4 shows the rate trend for the adsorption of Pb(II) ions onto the Co–Zn–Al–CO_3 LDH composite adsorbent. It was observed that the rate of removal of Pb(II) ions was very fast in the initial 10 min of commencing the experiment. Equilibrium was attained in 120 min. The initial fast rate of adsorption was attributed to adsorption on the readily available surface functional groups of the hydroxyl ions [19]. The subsequently slower rate may be ascribed to adsorption on the interior hydroxyl and carbonate anions, as well as entrapment of the Pb(II) ions within the composite pores [20].

To evaluate the mechanism of the Pb(II) adsorption process, the effect of time experimental data was analysed using five kinetic models – first-order, pseudo-first order, pseudo-second order, Elovich, and intra-particle diffusion kinetic models. Results (Table 1) showed that the poor fitting correlation coefficients (r^2 < 0.895) of the first-order, pseudo-first-order, and Elovich models suggested that the experimental data

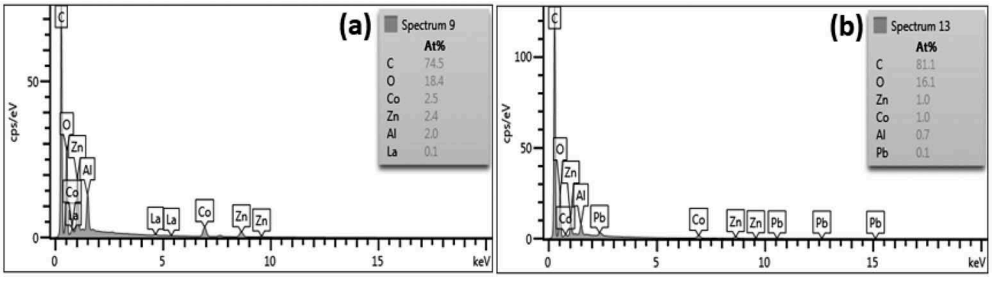

Figure 3. Energy dispersive X-ray spectroscopy of as the prepared Co–Zn–Al LDH (a) before and (b) after adsorption of Pb(II) ions.

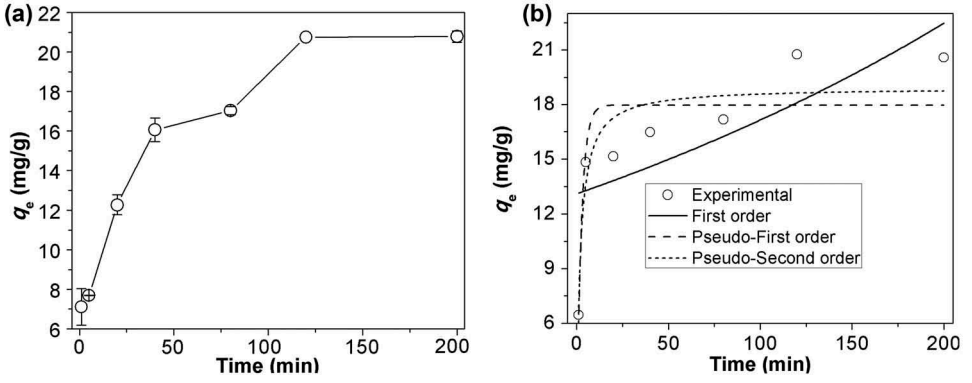

Figure 4. (a) Effect of time trend on the Pb(II) adsorption by Co–Zn–Al–CO_3 LDH (b) Nonlinear kinetic model fittings.

Table 1. Kinetic parameters of adsorption of Pb(II) by Co–Zn–Al LDH.

Kinetic model	Parameters	Linear
First-order	q_e (mg/g)	13.09
	k_1	–0.003
	r^2	0.539
Pseudo-first order	q_e (mg/g)	8.99
	k_2	0.023
	r^2	0.680
Pseudo-second order	q_e (mg/g)	21.28
	k_3	0.007
	r^2	0.993
Elovich	A	69.49
	β	0.416
	r^2	0.893
Intra-particle diffusion	C (mg/g)	9.93
	k_{IPD}	0.871
	r^2	0.745

cannot be described by these models. The pseudo-second-order r^2 was, however, very close to unity (≥0.993), and the estimated q_e value of the model was also close to the experimental data, and thus the model could be used to describe the experimental data. The model suggests that the Pb(II) ions' removal mechanism includes electrostatic interactions between the aqueous the Pb(II) ions and the active functional groups at the Co–Zn–Al–CO_3 LDH adsorption sites [1]. Figure 4(b) shows the nonlinear kinetic model fittings.

The Weber-Morris intra-particle diffusion kinetic model [11] has been used to determine the nature of the adsorption: whether surface or occurring within partitions/pores. The IPD model parameter C (mg/g) gives an idea of the estimated surface adsorption during the process; where the value is equal to experimental q_e value, then surface adsorption accounted for the bulk of Pb(II) removal from solution. For lower C values, the remaining values are attributed to partitioning within the adsorbent. The C value in this study was about half of the experimental q_e value; this indicates that both surface adsorption and partitioning of Pb(II) within the Co–Zn–Al–CO_3 LDH adsorbent occurred.

Effect of pH

To ascertain the adsorption property of the Co–Zn–Al–CO_3 LDH adsorbent, determining its adsorption response to changes in solution pH is vital. This is because pH affects the degree of charge density around both the adsorbent and adsorbate, and this in turn controls the extent of adsorption [21]. Hence, the effect of pH on Pb(II) adsorption has been tested. Figure 5 shows the result. From this, it is clear that the adsorption of Pb(II) on Co–Zn–Al–CO_3 LDH was pH dependent and increased with pH. The increase in adsorption with pH may be explained in terms of the ionisation states of the surface of the Co–Zn–Al–CO_3 LDH. Variation in pH causes either a protonation or deprotonation of the anionic surface adsorption sites depending on the prevailing pH. For instance, in acidic pH solution, the degree of the ionisation of the anionic surface adsorption sites (such as the hydroxyl and carbonates) is very low because of protonation. This resulted in reduced electrostatic interaction between the adsorption sites and the Pb(II) species in solution, and hence, the recorded low adsorption [22]. But at increasing or more alkaline pH, the once protonated anionic adsorption sites become *increasingly deprotonated* and negatively charged resulting in more electrostatic interaction and, consequently, higher adsorption (Figure 5).

Effect of concentration and temperature

Figure 6(a) shows the result of the effect of varying concentration on Pb(II) adsorption on Co–Zn–Al–CO_3 LDH. It was observed that increase in the concentration of Pb(II) ions in solution resulted in higher adsorption. This trend has been attributed to the fact that during adsorption, when the transport of Pb(II) ions between the composites' external surface film and internal pores are equal, cations will not be able to move across the boundary [23]. But an increase in concentration will re-initiate this movement especially into the pore spaces between the lamellae and may result in multi-layer adsorption, and thus the reported trend.

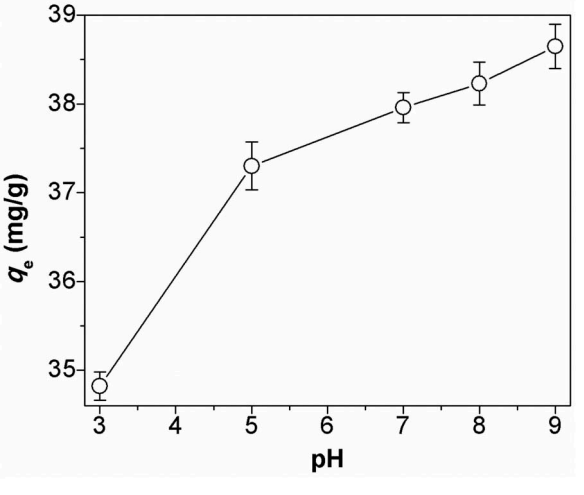

Figure 5. Effect of pH trend on the Pb(II) adsorption by Co–Zn–Al–CO_3 LDH.

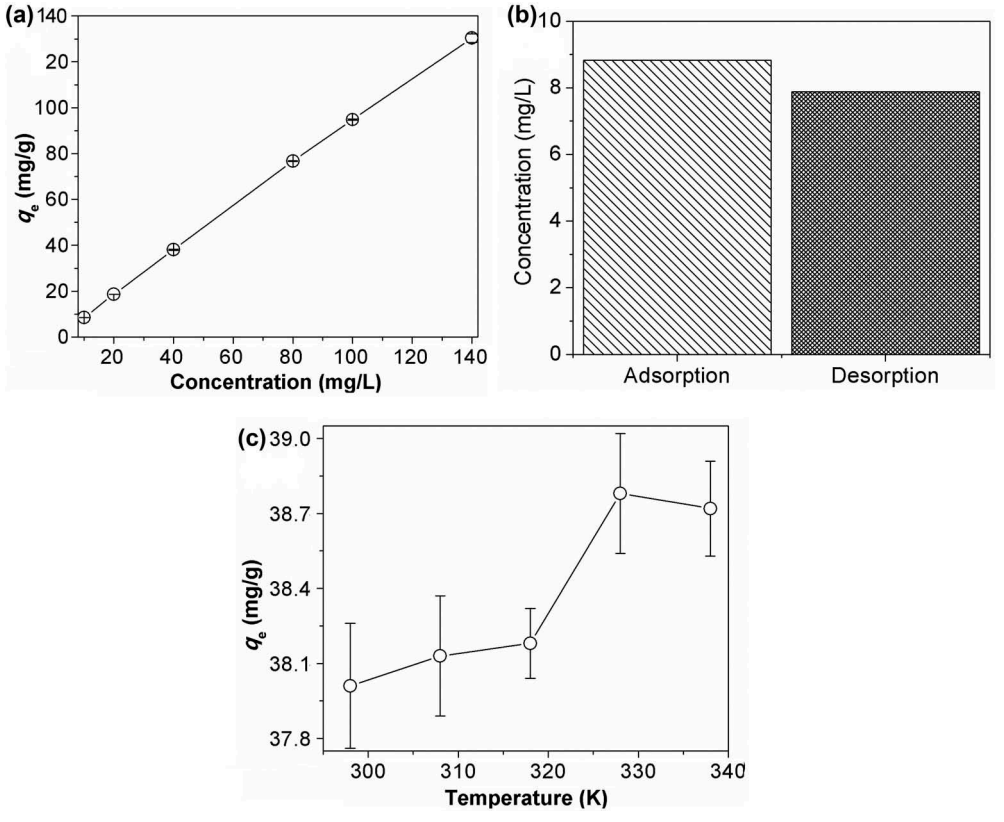

Figure 6. Effect of (a) concentration and (b) temperature trends on the Pb(II) adsorption by Co–Zn–Al–CO_3 LDH (c) Nonlinear adsorption isotherm model fittings.

Figure 6(b) shows the desorption experiment result. It is clear that approximately 90% of the adsorbed Pb(II) was desorbed. The desorption graph trend suggests that upon desorption, the adsorption sites and interstitial pores become vacant again for another round of Pb(II) adsorption. This indicates that the Co–Zn–Al–CO_3 LDH composite is reusable.

Figure 6(c) shows the effect of temperature on Pb(II) adsorption on the Co–Zn–Al–CO_3 LDH. The result showed that an increase in ambient temperature led to an increase in the aqueous Pb(II) ions adsorption. This trend suggested that the adsorption process was endothermic [24]. Thus, equilibrium data obtained at different temperatures were evaluated using the calculated thermodynamic parameters as shown in Table 2. The calculated

Table 2. Thermodynamic parameters of Pb (II) adsorption by Co–Zn–Al LDH.

Temperature (K)	ΔG° (kJ/mol)	ΔH° (kJ/K mol)	ΔS° (J/Kmol)	E_a (kJ/Kmol)
298	−0.176.5	0.097	79.9	16.0
308	−0.185.5			
318	−0.194.6			
328	−0.203.9			
338	−0.213.2			

positive $\Delta H°$ value confirmed the assumption that the Pb(II) adsorption process is endothermic, and the positive activation energy (E_a) obtained from the modified Arrhenius plot also supported this. The adsorption requires external energy input; hence, increase in solution temperature caused a reduction in adsorption for the cation. The $\Delta S°$ value for the adsorption process was positive, indicating increased randomness of the cations remaining in solution as the processes drifted towards equilibrium. The negative $\Delta G°$ values suggested spontaneous and feasible adsorption processes at all the temperatures studied.

Adsorption isotherm modelling

The Pb(II) equilibrium adsorption data were fitted to the Langmuir, Freundlich, Temkin, and Dubinin-Radushkevich adsorption isotherm models in order to understand the adsorption mechanism(s) in the Pb(II) removal process. Table 3 shows the calculated model parameters.

When the Langmuir and Freundlich adsorption isotherm parameters were compared, it was observed that the Freundlich adsorption isotherm model had a better or higher correlation coefficient ($r^2 \geq 0.821$). This suggests that the Freundlich adsorption isotherm model would describe the adsorption phenomenon better than the Langmuir. The better fit of the Pb(II) data to the Freundlich adsorption isotherm model implies that the adsorption process occurred on dissimilar surfaces of unequal energy with likely occurrence of Pb(II) multilayer on the surface of the Co–Zn–Al–CO_3 LDH at equilibrium. The n value is often regarded as an index of surface site energy distribution, and an n value less than unity represents non-linear adsorption on predominantly heterogeneous sites [23,25]. The calculated value of the Freundlich parameter n (<1) suggests that most isotherms in this adsorption process tended towards non-linearity. This is in agreement with the calculated IPD parameter C which indicated that the adsorption process was not solely a surface phenomenon but included both surface adsorption onto specific adsorption sites and partitioning within the pores of the Co–Zn–Al–CO_3 LDH.

The Temkin adsorption isotherm model takes into consideration the effects of some indirect adsorbate/adsorbate interactions on the adsorption isotherms. For this study, the model suggests that the heat of Pb(II) adsorption would decrease linearly as the process proceeds towards equilibrium. Although the Dubinin-Raduskevich adsorption

Table 3. Isotherm parameters of adsorption of Pb(II) by Co–Zn–Al LDH.

Isotherm	Parameters	Linear
Langmuir	Q_o (mg/g)	142.86
	b	0.072
	r^2	0.140
Freundlich	K_F (L/mg)	11.17
	$1/n$	1.33
	r^2	0.821
Temkin	B (J/mol)	61.65
	K_T (dm^3/g)	1.04
	r^2	0.980
Dubinin-Radushkevich	Q_D (mg/g)	122.01
	B_D (mol2/kJ^2)	4.5×10^{-7}
	E (kJ/mol)	3.33
	r^2	0.705

isotherm model did not appropriately ($r^2 \approx 0.705$) fit the adsorption data, the mean free energy E of adsorption per molecule of the adsorbate could give an idea of the nature of the adsorption process: whether physical or chemical. If the value is less than 40 kJ/mol, then it is physisorption; otherwise, it is regarded as chemisorption [26–28]. The value obtained for this study indicated that the adsorption process was a physical one.

The Pb(II) adsorption capacity of the synthesised Co–Zn–Al–CO_3 LDH was evaluated to compare its effectiveness with other LDH materials reported in the literature for Pb(II) adsorption (Table 4). It was observed that the ternary LDH performed better than all pristine binary LDH adsorbents as well as most intercalated derivatives reported in the literature. The adsorption capacity was also comparable to some of the best performing intercalated derivatives as well. This is an indication that ternary LDH adsorbents, as well as their derivatives, may be effective for Pb(II) removal from aqueous solutions.

Following the success of the desorption experiment (Figure 6(b)) which indicated that the Co–Zn–Al–CO_3 LDH composite is reusable, the next stage of the study will be to examine the adsorbent in detail for treating real wastewater samples. The preliminary experiments indicate the applicability of this adsorbent with regard to Vaal River water.

The Co–Zn–Al–CO_3 LDH composite from the study will be applied to column studies using simulated contaminated water in order to determine the optimum parameters and conditions for such column adsorption. This will be followed by replacement of the simulated contaminated water with actual polluted water from the Vaal River. The river is a major source of water for the Emfuleni municipality in South Africa, but it is also a health risk for the consumers, as it has been heavily polluted by effluents from several mining, agricultural and construction companies in this highly industrialised area of South Africa. The pollution has killed fishes in the river. LDH can undoubtedly help to treat the Vaal River.

Conclusion

A ternary layered double hydroxide intercalated with carbonate (Co–Zn–Al–CO_3 LDH) was synthesised by the co-precipitation method. The FTIR result showed the presence of hydroxyl groups and the intercalated carbonate anions within the well-defined LDH crystal structure. The TGA-DTA results confirmed the presence of these anionic groups which were liberated from the LDH structure at approximately 200°C and 300°C, respectively. The LDH-specific surface area, pore

Table 4. Comparison of adsorption capacity of the synthesised ternary LDH with those of pristine binary and their intercalated derivatives for Pb(II) adsorption.

Adsorbent	Pb qe (mg/g)	References
Mg_2Al LDH	66.2	[29]
Mg_2Al-Cl LDH	40	[30]
Mg_2Al-DTPA LDH*	170	[30]
Mg_2Al-EDTA LDH	211.6	[31]
Zn_2Al-$N0_3$-DPTA LDH*	145.0	[32]
Zn_2Al-$N0_3$-DMSA LDH*	414.4	[32]
Mg_2Al-humate anion LDH	99.5	[33]
Co–Zn–Al–CO_3 LDH	130.3	This study

*DTPA – Diethylene triamine penta-acetic acid; DMSA – Meso-2,3-dimercapto-succinic acid.

diameter and width are 54.0 m^2/g, 41.3 and 25.1 nm, respectively. The Pb(II) adsorption equilibrium was achieved in 120 min, and adsorption increased with concentration and temperature. A Pb(II) adsorption capacity of 130.34 mg/g could be reached for this LDH. The pseudo-second-order kinetic model suggested that the adsorption process was mainly electrostatic. The intra-particle diffusion model indicated that the bulk of the adsorption occurred within the pores rather than the surface. The Freundlich adsorption isotherm model indicated that both the hydroxyl and carbonate were active in the Pb(II) adsorption process which was spontaneous and endothermic. The desorption test suggested that approximately 90% of the adsorbed Pb(II) could be desorbed; hence, the Co–Zn–Al–CO_3 LDH may be reused.

Acknowledgements

This study was supported by the Vaal University of Technology Postdoctoral Research grant of 2017.

Disclosure statement

No potential conflict of interest was reported by the authors.

Funding

This study was supported by the Vaal University of Technology Postdoctoral Research grant of 2017.

References

[1] Olu-Owolabi, B.I., Alabi, A.H., Diagboya, P.N., Unuabonah, E.I., and During, R.A., 2017, Adsorptive removal of 2,4,6-trichlorophenol in aqueous solution using calcined kaolinite-biomass composites. *Journal of Environmental Management* **192**, 94–99. doi: 10.1016/j.jenvman.2017.01.055

[2] Olu-Owolabi, B.I., Diagboya, P.N., Unuabonah, E.I., Alabi, A.H., Düring, R.A., and Adebowale, K.O., 2018, Fractal-like concepts for evaluation of toxic metals adsorption efficiency of feldspar-biomass composites. *Journal of Cleaner Production* **171C**, 884–891. doi: 10.1016/j.jclepro.2017.10.079

[3] Yu, Y., Yu, L., and Paul Chen, J., 2015, Adsorption of fluoride by Fe–Mg–La triple-metal composite: adsorbent preparation, illustration of performance and study of mechanisms. *Chemical Engineering Journal* **262**, 839–846. doi: 10.1016/j.cej.2014.09.006

[4] Wang, X., Zhu, X., and Meng, X., 2017, Preparation of a Mg/Al/Fe layered supramolecular compound and application for removal of Cr(VI) from laboratory wastewater. *RSC Advances* **7**, 34984. doi: 10.1039/C7RA04646D

[5] Mahjoubi, F.Z., Khalidi, A., Abdennouri, M., and Barka, N., 2017, Zn–Al layered double hydroxides intercalated with carbonate, nitrate, chloride and sulphate ions: synthesis, characterisation and dye removal properties. *Journal of Taibah University for Science* **11**, 90–100. doi: 10.1016/j.jtusci.2015.10.007

[6] Diagboya, P.N. and Dikio, E.D., 2018, Dynamics of mercury solid phase extraction using Barbula lambarenensis. *Environmental Technology and Innovation* **9**, 275–284. doi: 10.1016/j.eti.2018.01.002

[7] Diagboya, P.N. and Dikio, E.D., 2018, Silica-based mesoporous materials; emerging designer adsorbents for aqueous pollutants removal and water treatment. *Microporous Mesoporous Materials* **266C**, 252–267. doi: 10.1016/j.micromeso.2018.03.008

[8] Zou, Y., Wang, X., Wu, F., Yu, S., Hu, Y., Song, W., Liu, Y.H., Wang, H., Hayat, T., and Wang, X.K., 2016, Controllable synthesis of Ca-Mg-Al layered double hydroxides and calcined layered double oxides for the efficient removal of U(VI) from wastewater solutions. *ACS Sustainable Chemisry and Engineering* **5**, 1173–1185. doi: 10.1021/acssuschemeng.6b02550

[9] Qu, J., He, X., Chen, M., Huang, P., Zhang, Q., and Liu, X., 2017, A facile mechanochemical approach to synthesize Zn-Al layered double hydroxide. *Journal of Solid State Chemistry* **250**, 1–5. doi: 10.1016/j.jssc.2017.03.013

[10] Kovanda, F., Grygar, T., Dornicak, V., Rojka, T., Bezdicka, P., and Jiratova, K., 2005, Thermal behaviour of Cu–Mg–Mn and Ni–Mg–Mn layered double hydroxides and characterization of formed oxides. *Applied Clay Science* **28**, 121–136. doi: 10.1016/j.clay.2004.01.007

[11] Weber, W.J. and Morris, J.C., 1963, Kinetics of adsorption on carbon from solutions. *Journal of Sanitary Engineering Division. American Society of Civil Engineers* **89**, 31–60.

[12] Ayawei, N., Ekubo, A.T., Wankasi, D., and Dikio, E.D., 2015, Adsorption dynamics of copper(II) on ZnFe layered double hydroxide. *European Journal of Scientific Research* **130**, 235–248.

[13] Jiao, F.P., Fu, Z.D., Shuai, L., and Chen, X.Q., 2012, Removal of phenylalanine from water with calcined CuZnAl-CO3 layered double hydroxides. *Transactions of Nonferrous Metals Society of China* **22**, 476–482. doi: 10.1016/S1003-6326(11)61201-6

[14] Benício, L.P.F., Silva, R.A., Lopes, J.A., Eulálio, D., Santos, R.M.M., Aquino, L.A., Vergütz, L., Novais, R.F., Costa, L.M., Pinto, F.G., and Tronto, A.J., 2015, Layered double hydroxides nanomaterials for applications in agriculture. *Revista Brasileira de Ciência do Solo* **39**, 1–13. doi: 10.1590/01000683rbcs2015081

[15] Starukh, G., 2017, Photocatalytically enhanced cationic dye removal with Zn-Al layered double hydroxides. *Nanoscale Research Letters* **12**, 391. doi: 10.1186/s11671-017-2173-y

[16] Carja, G., Nakamura, R., Aida, T., and Niiyama, H., 2001, Textural properties of layered double hydroxides: Effect of magnesium substitution by copper or iron. *Microporous and Mesoporous Materials* **47**, 275–284. doi: 10.1016/S1387-1811(01)00387-0

[17] Gabor, A., Davidescu, C.M., Negrea, A., Ciopec, M., and Lupa, L., 2015, Behaviour of silica and florisil as solid supports in the removal process of as(v) from aqueous solutions. *Journal of Analytical Methods in Chemistry* **2015**, 562780. doi: 10.1155/2015/562780

[18] Srankó, D., Sipiczki, M., Bajnóczi, É.G., Darányi, M., Kukovecz, Á., Kónya, Z., Canton, S. E., Norén, K., Sipos, P., and Pálinkó, I., 2011, A SEM, EDX and XAS characterization of Ba (II)Fe(III) layered double hydroxides. *Journal of Molecular Structure* **993**, 62–66. doi: 10.1016/j.molstruc.2010.10.004

[19] Okoli, C.P., Diagboya, P.N., Anigbogu, I.O., Olu-Owolabi, B.I., and Adebowale, K.O., 2016, Competitive biosorption of Pb(II) and Cd(II) ions from aqueous solutions using chemically modified moss biomass (Barbula lambarenensis). *Environmental Earth Sciences*, **76**, 33–42. doi: 10.1007/s12665-016-6368-9

[20] Diagboya, P.N., Olu-Owolabi, B.I., and Adebowale, K.O., 2014, Microscale scavenging of pentachlorophenol in water using amine and tripolyphosphate-grafted SBA-15 silica: batch and modeling studies. *Journal of Environmental Management* **146**, 42–49. doi: 10.1016/j.jenvman.2014.04.038

[21] Diagboya, P.N., Olu-Owolabi, B.I., Zhou, D., and Han, B.H., 2015, Graphene oxide–Tripolyphosphate hybrid used as a potent sorbent for cationic dyes. *Carbon* **79**, 174–182. doi: 10.1016/j.carbon.2014.07.057

[22] Olu-Owolabi, B.I., Alabi, A.H., Unuabonah, E.I., Diagboya, P.N., Böhm, L., and Düring, R. A., 2016, Calcined biomass-modified bentonite clay for removal of aqueous metal ions. *Journal of Environmental Chemical Engineering* **4**, 1376–1382. doi: 10.1016/j.jece.2016.01.044

[23] Olu-Owolabi, B.I., Diagboya, P.N., and Adebowale, K.O., 2014, Evaluation of pyrene sorption–Desorption on tropical soils. *Journal of Environmental Management* **137**, 1–9. doi: 10.1016/j.jenvman.2014.01.048

[24] Diagboya, P.N., Olu-Owolabi, B.I., Dikio, E.D., and Adebowale, K.O., 2018, Concentration-dependent and simultaneous sorption and desorption of pyrene and fluorene on major soil minerals in sub-Saharan Africa. *Applied Clay Science* **153**, 257–264. doi: 10.1016/j.clay.2017.11.037

[25] Weber, W.J., Jr., McGinley, P.M., and Katz, L.E., 1992, A distributed reactivity model for sorption by soils and sediments: 1. Conceptual basis and equilibrium assessments. *Environmental Science and Technology* **26**, 1955–1962. doi: 10.1021/es00034a012

[26] Horsfall, M., Spiff, A.I., and Abia, A.A., 2004, Studies on the influence of mercapto acetic acid(MAA) modification on cassava(Manihot esculenta cranz) waste biomass on the adsorption of Cu^{2+} and Cd^{2+} from aqueous solution. *Bulletin of Korean Chemical Society* **25**, 969–976. doi: 10.5012/bkcs.2004.25.7.969

[27] Lodeiro, P., Barriada, J.L., and Herrero, R., 2006, Sastre-Vicente: The marine macroalgae cystoserira baccata as biosorbent for cadmium (II) and lead (II) removal: Kinetic and equilibrium studies. *Environmental Pollution* **142**, 264–273. doi: 10.1016/j.envpol.2005.10.001

[28] Sarı, A., Tuzen, M., and Soylak, M., 2007, Adsorption of Pb(II) and Cr(III) from aqueous solution on celtek clay. *Journal of Hazardous Materials* **144**, 41–46. doi: 10.1016/j.jhazmat.2006.09.080

[29] Zhao, D., Sheng, G., Hu, J., Chen, C., and Wang, X., 2011, The adsorption of Pb(II) on Mg2Al layered double hydroxide. *Chemical Engineering Journal* **171**, 167–174. doi: 10.1016/j.cej.2011.03.082

[30] Liang, X., Hou, W., Xu, Y., Sun, G., Wang, L., Sun, Y., and Qin, X., 2010, Sorption of lead ion by layered double hydroxide intercalated with diethylenetriaminepentaacetic acid. *Colloids and Surfaces A: Physicochemical and Engineering Aspects* **366**, 50–57. doi: 10.1016/j.colsurfa.2010.05.012

[31] Pérez, M.R., Pavlovic, I., Barriga, C., Cornejo, J., Hermosín, M.C., and Ulibarri, M.A., 2006, Uptake of Cu^{2+}, Cd^{2+} and Pb^{2+} on Zn–Al layered double hydroxide intercalated with EDTA. *Applied Clay Science* **32**, 245–251. doi: 10.1016/j.clay.2006.01.008

[32] Pavlovic, I., Pérez, M.R., Barriga, C., and Ulibarri, M.A., 2009, Adsorption of Cu^{2+}, Cd^{2+} and Pb^{2+} ions by layered double hydroxides intercalated with the chelating agents diethylenetriaminepentaacetate and meso-2,3-dimercaptosuccinate. *Applied Clay Science* **43**, 125–129. doi: 10.1016/j.clay.2008.07.020

[33] González, M.A., Pavlovic, I., Rojas-Delgado, R., and Barriga, C., 2014, Removal of Cu^{2+}, Pb^{2+} and Cd^{2+} by layered double hydroxide–Humate hybrid. Sorbate and sorbent comparative studies. *Chemical Engineering Journal* **254**, 605–611. doi: 10.1016/j.cej.2014.05.132